III. RESULTS

Mass numbers for the fission fragments of ^{252}Cf have a value such that $90 \leq m \leq 160$. The resulting stopping-power plots as obtained by successive application of Eqs. (2) and (4) and normalizing to the velocity of the most probable light fragment are shown in Figs. 2–4. In some cases such as on the boundaries and in the mid-region of the mass range, the resulting energy points were not available due to poor statistics in the raw experimental data. The bromine and iodine ion data, as obtained by Moak *et al.*,[9] shown on the same plots are in reasonable agreement for all materials.

Figures 5–7 show the results of the normalized stopping cross sections as a function of the projectile atomic number Z_1. Included on the graphs are points obtained by Moak *et al.*[9] and the theoretical prediction by Lindhard *et al.*[3] The solid line is from the empirical relationship mentioned earlier.[10] The errors in the data resulting from a statistical uncertainity are estimated to be about 25–30% full width at half-maximum (FWHM) for Au and Ag and somewhat larger for C. Analysis of the raw data was rather involved making precise estimates of the errors difficult. The maximum probable error in the mass determination was about 4 amu. Thus the choice of the size of mass bin was 5 amu. An inspection of the figures will show that the data are consistant with the estimated errors.

The characteristic behavior of the Au and Ag data indicates that the theory is incomplete especially for the high-mass fragments. Statistical uncertainties in the carbon data prevent the drawing of any definite conclusions. One possible reason for the discrepancies is that internal excitation is not accounted for in the theory and may be much greater in the heavier ions.

†Research supported by the U. S. Atomic Energy Commission.

*Much of this material is contained in a Master's thesis by one of the authors (A. W.) as submitted to the Graduate School, Murray State University.

[1]N. Bohr, Kgl. Danske Videnskab. Selskab, Mat.-Fys. Medd. 18, No. 8 (1948).

[2]J. Lindhard, M. Scharff, and H. E. Schiott, Kgl. Danske Videnskab. Selskab, Mat.-Fys. Medd. 33, No. 14 (1963).

[3]C. D. Moak, H. O. Lutz, L. B. Bridwell, L. C. Northcliffe, and S. Datz, Phys. Rev. 176, 427 (1968).

[4]J. B. Cumming and V. P. Crespo, Phys. Rev. 161, 287 (1967).

[5]W. Whaling, *Handbuch der Physik* (Springer-Verlag, Berlin, 1958), Vol. 34, p. 193.

[6]J. Asbell (unpublished); L. Bridwell and L. M. Beyer, Bull. Am. Phys. Soc. 13, 1444 (1968).

[7]H. W. Schmitt, W. M. Gibson, J. H. Neiler, F. J. Walter, and J. D. Thomas, *Proceedings of the Symposium on the Physics and Chemistry of Fission, Salzburg*, 1965 (International Atomic Energy Agency, Vienna, Austria, 1965).

[8]L. B. Bridwell, L. C. Northcliffe, S. Datz, C. D. Moak, and H. O. Lutz, Bull. Am. Phys. Soc. 12, 28 (1967).

[9]C. D. Moak and M. D. Brown, Phys. Rev. 149, 244 (1966).

[10]L. Bridwell and C. D. Moak, Phys. Rev. 156, 242 (1967).

[11]L. E. Glendenin and J. P. Unik, Phys. Rev. 140, B1301 (1965).

PHYSICAL REVIEW B VOLUME 3, NUMBER 7 1 APRIL 1971

Electron Paramagnetic Resonance of Mn^{2+} in $KTaO_3$

David M. Hannon
IBM Research Laboratory, San Jose, California 95114
(Received 9 September 1970)

The electron paramagnetic resonance of Mn^{2+} in $KTaO_3$ was measured over a temperature range 4–110 K. At 77 K, the spin-Hamiltonian constants are $g_{\parallel} = 2.000 \pm 0.001$, $g_{\perp} = 2.000 \pm 0.001$, $D = +0.147 \pm 0.003$ cm^{-1}, $A_{\parallel} = -(86.5 \pm 0.5) \times 10^{-4}$ cm^{-1}, $A_{\perp} = -(84 \pm 1.5) \times 10^{-4}$ cm^{-1}. The results indicate that the Mn^{2+} is substitutional at a Ta^{5+} site with an adjacent oxygen vacancy. The temperature dependence of D is correlated with the soft-mode frequency of the host. The quadrupole splitting $Q' = +(0.8 \pm 0.1) \times 10^{-4}$ cm^{-1} was determined from the forbidden hyperfine transitions.

I. INTRODUCTION

This paper presents the electron paramagnetic resonance (EPR) of Mn^{2+} in the cubic perovskite $KTaO_3$, and is the first of two papers describing the spectroscopy of manganese in this host. It is

convenient to separate the EPR from the optical-spectroscopy results because they arise from different valence states: the EPR from Mn^{2+} and the optical properties from Mn^{3+}.[1]

The EPR of Mn^{2+} and of isoelectronic Fe^{3+} in perovskite hosts have been extensively studied.[2–13] The results of such studies can be divided into two categories: First, the determination of the impurity site and immediate surroundings; and second, the effects of phase transitions and soft modes of the host crystal on the EPR. The most interesting example of the second category is $SrTiO_3:Fe^{3+}$, where the rotation of the TiO_6 octahedra is observed in the EPR rotation spectra.[5,6] This rotation is the order parameter of the 110 K phase transition.[5] Above the phase transition, the effect of the soft zone-center mode on the cubic-field constant can be seen.[4]

Here, we describe the EPR of Mn^{2+} in $KTaO_3$ and conclude that the Mn^{2+} occupies the Ta^{5+} site with an adjacent oxygen vacancy. We suggest that the temperature variation of the axial constant D (caused by the oxygen vacancy) reflects an interaction with the host soft mode. However, a discussion of such an interaction must be very qualitative because neither reliable theoretical calculations[14,14a] of D nor a convenient description of the effect of the soft mode on the impurity is available.

The hyperfine transitions, allowed and forbidden, are used to calculate the hyperfine constants and the nuclear quadrupole splitting.

II. RESULTS

A. Spin Resonance

The method of crystal growth is described elsewhere.[13] No effects of concentration were seen for impurity concentration variation of about an order of magnitude. The EPR was recorded at 77 K and below. Above 77 K, the lines begin to broaden and are not seen at room temperature, a somewhat surprising result since Mn^{2+} EPR is usually seen at room temperature and higher.

Figure 1 gives the frequency vs magnetic field for the field along the [100] direction. Each line, which represents a sextet of hyperfine lines, has our assignment indicated. We use the strong field quantum numbers and use $\parallel$ and $\perp$ to mean that the field is parallel or perpendicular to the axial crystal field. Some of the forbidden transitions, such as the $(-\frac{1}{2} \rightarrow +\frac{5}{2})_\perp$ transition, have considerable intensity due to the large crystal field. The $(\frac{1}{2} \rightarrow -\frac{1}{2})_\parallel$

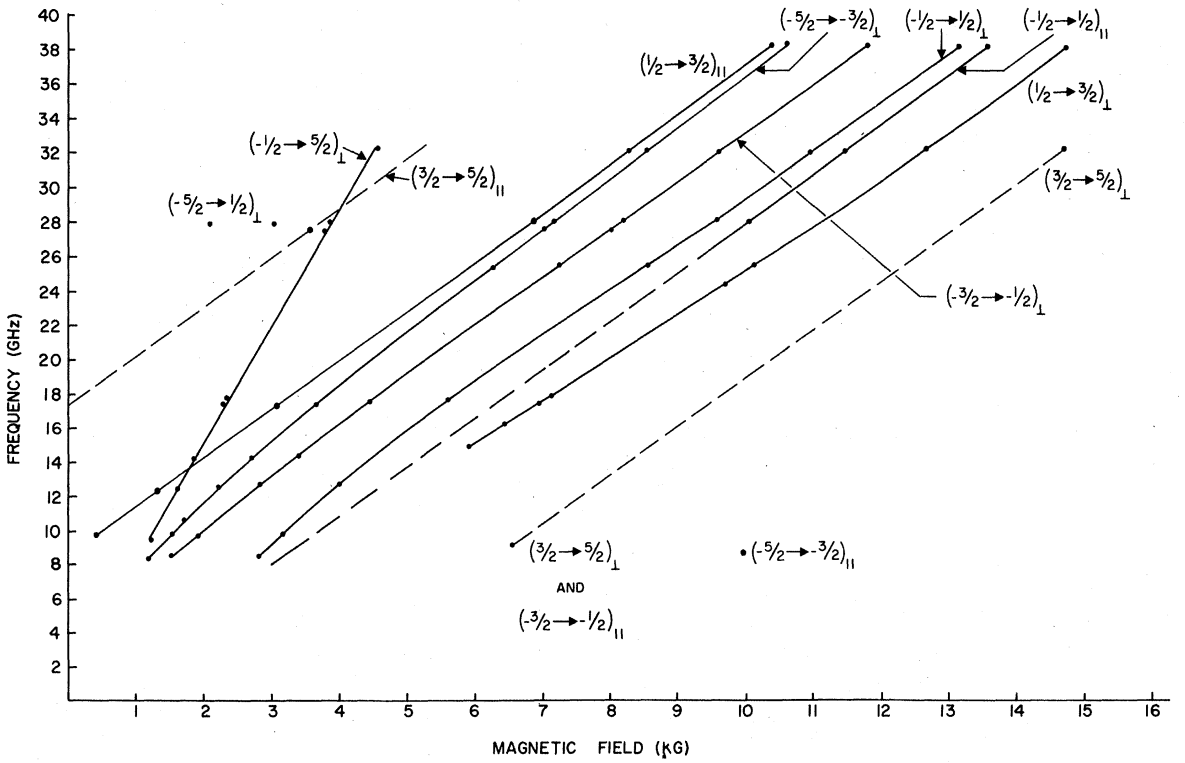

FIG. 1. Frequency vs magnetic field for $\vec{H}$ parallel to a $\langle 100 \rangle$ axis. The lines connect the data points and are characterized by the strong field quantum numbers of the assigned transition. Broken lines for the $(\frac{3}{2} \rightarrow \frac{5}{2})_\parallel$ and the $(\frac{3}{2} \rightarrow \frac{5}{2})_\perp$ transitions are used to indicate that only one or two data are available for these transitions. The reason for the broken line for the $(-\frac{1}{2} \rightarrow \frac{1}{2})_\parallel$ transition is discussed in the text.

sextet is shown with a broken line to indicate that below about 20 GHz we were unable to resolve a sextet of lines. We discuss this in the section on hyperfine transitions.

Complete field rotation data are not available because the hyperfine lines tend to broaden and the splittings between hyperfine lines increase rapidly as the field is rotated. From *et al.*[15] discuss this behavior which is caused by the mixing of the hyperfine levels by the large axial field. The linewidths vary between 12 and 20 G except for the $(\frac{1}{2} \rightarrow -\frac{1}{2})_{\parallel}$ sextet which is 6 G wide. The minimum width is probably caused by the nuclear moment of the potassium ions which contribute about 60 G to the width of Fe^{3+} in $KTaO_3$.[13]

The data of Fig. 1 are fitted by the usual axial spin Hamiltonian for[16] d^5:

$$H = g_{\parallel}\mu_B H_z S_z + g_{\perp}\mu_B(H_x S_x + H_y S_y) + D(S_z^2 - \tfrac{35}{12}) + (\text{quartic terms in } a, F) + A S_z I_z + B(S_x I_x + S_y I_y) - \gamma\beta_n \vec{H}\cdot\vec{I} + Q'(I_z^2 - \tfrac{35}{12}) .$$

The $(-\frac{1}{2} \rightarrow \frac{1}{2})_{\parallel}$ sextet determines the $g_{\parallel}$ value and the parallel manganese hyperfine interaction constant:

$$g_{\parallel} = 2.000 \pm 0.001 ,$$

$$A_{\parallel} = -(86.5 \pm 0.5)\times 10^{-4}\ \text{cm}^{-1} .$$

To find D, and also $g_{\perp}$ and $A_{\perp}$, we solved a 36 $\times$36 matrix for $H \perp D$ with 18 lines as input, these perpendicular lines being more intense in the spectrum. The results are

$$D = +0.147 \pm 0.003\ \text{cm}^{-1} ,$$

$$g_{\perp} = 2.000 \pm 0.001 ,$$

$$A_{\perp} = -(84 \pm 1.5)\times 10^{-4}\ \text{cm}^{-1} .$$

The calculation for the quartic constants (a, F) gives a very small negative result but with a relatively large error. Since D is so much larger than the quartic constants, we cannot obtain a reliable value from the computer diagonalization and consequently do not quote a value for $a - F$. The sign of D is determined by comparing intensities at different temperatures. The sign of the product AD is determined from the forbidden hyperfine transitions with the result that A is negative as expected. With the parameters given, all of the EPR lines are accounted for. Therefore, the Mn^{2+} has only one site, or, if you wish, three equivalent sites with an axial field along each of the $\langle 100 \rangle$ directions.[17]

B. Site Choice

Although the site determination is not unequivocal, we now argue that the Mn^{2+} ion is substitutional for the Ta^{5+} with an adjacent oxygen vacancy. Considering the direction of the axial distortion and the size of Mn^{2+}, the only alternate possibility is the dodecahedral K^{1+} site. $KTaO_3$ tends to grow with oxygen deficiencies,[13,18] which favors a reduction in cation charge, and, therefore, substitution at the Ta^{5+} site is favored over the K^{1+} site. Note that a Mn^{2+} + oxygen vacancy center would have an equivalent 4+ charge when substituted for Ta^{5+}. It is known that quadrivalent ions such as Ti^{4+} and Sn^{4+} are readily incorporated into $KTaO_3$.[13,18]

To estimate whether the magnitude of D is reasonable for our assignment, we consider equivalent systems where D is known for both Mn^{2+} and Fe^{3+}. Table I gives four systems where the axial distortion varies from a stress perturbed cubic system (MgO) to the strongly distorted $PbTiO_3$ and $KTaO_3$. Note that the ratio D_{Fe}/D_{Mn} increases with increasing distortion. Since the D ratios in the two strongly distorted systems, viz., $PbTiO_3$ and $KTaO_3$ with an oxygen vacancy, are the same, we conclude that the magnitude of D is compatible with the site assignment. We should also point out that the size of Mn^{2+} is closer to Ta^{5+} than to K^{1+}, although we feel that arguments based on relative size of the ions are not overly convincing.

The magnitude of the hyperfine constant can be useful in choosing between the Ta^{5+} octahedral site and the K^{1+} dodecahedral site. $A_{\perp}$ in our case is quite close to the $A_{\perp}$ reported for Mn^{2+} in[8] $BaTiO_3$ and $PbTiO_3$,[8] both of which are assigned to the octahedral Ti^{4+} site. Simanek and Müller[19] have discussed the hyperfine constant and show that A can be considered as a function of only the type of ligand and the coordination. Our hyperfine constant is

TABLE I. Axial constant D for Fe^{3+} and Mn^{2+} in various host lattices.

Host	$D_{Fe}(\text{cm}^{-1})$	$D_{Mn}(\text{cm}^{-1})$	Ratio	Comment	Ref.
MgO	0.039×10^{-4}	0.011×10^{-4}	3.7	D/(unit stress)	14
$BaTiO_3$	0.093	0.021	4.4	1% ferroelectric distortion	2, 7
$PbTiO_3$	0.53	0.05	10	6% ferroelectric distortion	12, 8
$KTaO_3$	1.44	0.144	10	Oxygen vacancy	11, present paper

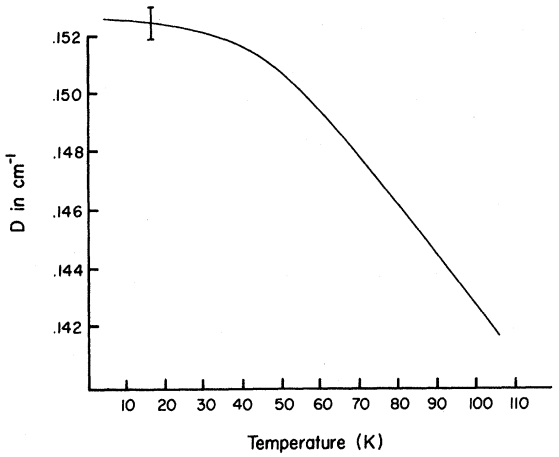

FIG. 2. D vs temperature for Mn^{2+} in $KTaO_3$. The solid line simply connects data points. The error bar is used to indicate relative error and applies to the full range of D.

somewhat higher than their prediction for an octahedral site with oxygen ligands, which may be due to the strong distortion in our case.

The effect of codoping with Ti and Mn is of interest. Crystals with Mn and Ti show no Mn EPR although the optical properties are essentially the same as those of Mn-doped crystals.[1] In Ref. 13, we demonstrated that titanium inhibited Fe^{3+} from occupying the Ta^{5+} site in $KTaO_3$ and here we give evidence that titanium has the same effect on Mn^{2+}.

C. Temperature Dependence of D

Figure 2 gives the temperature dependence of D up to 110 K. The line is a smooth curve drawn through data points. The error bar indicates a relative error and is less than the absolute error of D. Above 110 K the hyperfine lines become too broad to measure. The temperature dependence of the hyperfine constant has not been measured. Figure 2 shows the D constant increasing roughly linearly as the temperature is decreased from 110 to about 50 K, below which D tends to become independent of temperature.

We suspect that the D variation reflects an interaction with the soft mode mainly because of the large change of D at these low temperatures. D changes by ~7% below 100 K, whereas, D is temperature independent below 100 K for axial Cr^{3+} in[20] MgO and for Fe^{3+} in Al_2O_3.[21] However, D does exhibit considerable temperature change at low temperature for Fe^{3+} in[12,22] $SrTiO_3$ and in[12,23] $PbTiO_3$; in both cases D is associated with a phase transition.

To further support the idea of a soft-mode interaction, we note that the temperature dependence of both D and ω "rounds off" below ~50 K.[24] In fact, a plot of D vs ω_{TO}^2 is linear, within experimental accuracy, with a negative slope. A soft-mode interaction has been convincingly demonstrated for Gd^{3+} in[4] $SrTiO_3$ where the Gd^{3+} substitutes for the Sr^{2+} and the cubic symmetry is retained. The temperature dependence of the cubic-field constant b_{40} is proportional to $1/(T-T_c)$ or to $1/\omega_{TO}^2$ where ω_{TO} is the soft-mode frequency. For this case, the Gd^{3+} is considered an effective +1 charge which attracts the 12 oxygen neighbors toward the Gd thereby increasing b_{40}. Each normal mode of the lattice makes a contribution to the oxygen displacement proportional to $1/\omega^2$. Since only the soft mode is temperature dependent, the cubic-field constant has a temperature dependence proportional to $1/\omega_{TO}^2$.

Contrary to the case of Gd^{3+} in $SrTiO_3$, we are not able to formulate a useful model to explain the D variation of Fig. 2. To arrive at such a model would require three steps: (i) determine the positions of the ions around the Mn^{2+} impurity; (ii) estimate the effect of a soft mode on the ion positions; and (iii) calculate D from the ion positions. At present none of these steps can be accomplished with any degree of confidence. Attempts at calculating D from ionic positions have been rather discouraging.[14a,25]

D. Hyperfine Structure

Figure 3 shows two hyperfine sextets recorded at 27.2 GHz. Both are the $-\frac{1}{2}\rightarrow\frac{1}{2}$ transition; for the lower one $\vec{H}$ is perpendicular to the axial distortion and for the upper one $\vec{H}$ is parallel to the axial distortion. The prominent doublets between the hyperfine lines on the upper sextet are the so-called forbidden transitions, that is, transitions where the nuclear magnetic quantum number changes by ± 1. Forbidden doublets can also be seen on the lower sextet.

The intensity of the forbidden lines is given by[26]

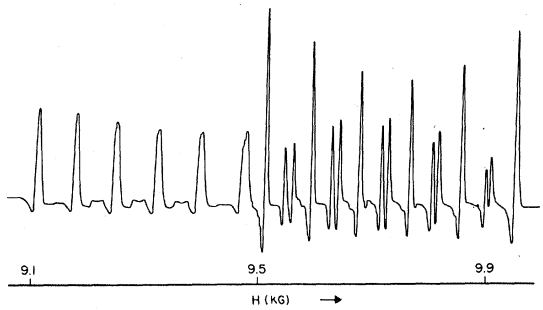

FIG. 3. Hyperfine structure of Mn^{2+} in $KTaO_3$. Lower sextet is the $(-\frac{1}{2}\rightarrow\frac{1}{2})_\perp$ transition. Upper sextet is the $(-\frac{1}{2}\rightarrow\frac{1}{2})_\parallel$ transition. Forbidden doublets are seen on both sextets.

$$\frac{I_f}{I_0}=\left(\frac{3D\sin 2\theta}{4g\mu_B H}\right)^2\left\{1+\frac{S(S+1)}{3M(M-1)}\right\}^2\{I(I+1)-m^2+m\}, \tag{1}$$

where I_f is the forbidden intensity and I_0 is the allowed intensity. Of course, Eq. (1) is limited by the condition $I_f/I_0<1$. Equation (1) yields a rough estimate of D in agreement with the value listed above. The angle θ for Fig. 3 is about 2°. At 6° the $\Delta m=2$ transitions are evident as splittings of the $\Delta m=0$ lines. Note that the last factor of Eq. (1) gives the 5 : 8 : 9 : 8 : 5 intensity variation across the forbidden doublets in agreement with Fig. 3.

We have mentioned that the $(-\frac{1}{2}\rightarrow\frac{1}{2})_{\parallel}$ spectrum at X band is not a sextet of lines but rather a group of lines centered at $g=2$ without an obvious pattern. Apparently, the hyperfine levels are strongly perturbed in this region. The source of the perturbation is probably the off-diagonal hyperfine term $\frac{1}{2}B(S_+I_-+S_-I_+)$ which mixes states with spin quantum numbers differing by 1. Since the $M_s=-\frac{3}{2}$ level crosses the $M_s=-\frac{1}{2}$ level at $g\mu_B H=2D$, the $M_s=-\frac{1}{2}$ hyperfine states will be strongly mixed in the X-band region.

The separation between forbidden doublets, for $\theta\simeq 0$, is given by[26,27]

$$\Delta H=\frac{17B^2}{2H_0}+\frac{\gamma\beta_n}{g\mu_B}[2H_0-A(2m-1)]+\frac{16A^2D^2}{H_0^3}-(3\cos^2\theta-1)\left(Q'-\frac{4A^2D}{H_0^2}\right)(2m-1)+\frac{16DA^3}{H_0^3}[\tfrac{27}{4}+m-m^2], \tag{2}$$

where we have omitted terms obviously too small to contribute. m ranges from $-\frac{3}{2}$ to $+\frac{5}{2}$ in this formulation of the doublet splitting.

The forbidden lines in Fig. 3 are 6 G wide and tend to overlap as the splitting decreases. For this reason we fit Eq. (2) using the largest and most accurate splitting, rather than the difference between $\Delta H(-\frac{3}{2})$ and $\Delta H(+\frac{5}{2})$.[27] Since A is negative, the largest splitting occurs for $m=-\frac{3}{2}$. Solving Eq. (2) with $\Delta H(-\frac{3}{2})=17.0\pm0.8$ G, we find

$$Q'=+0.9\pm0.1\ \text{G}=+(0.8\pm0.1)\times10^{-4}\ \text{cm}^{-1}.$$

Sroubek *et al.*[28] measured the stress-induced nuclear quadrupole splitting for Mn^{2+} in MgO and compared the measured Q' with a calculation of Q' from the formula $Q'=3Qq(1-\gamma_\infty)/4I(2I-1)$. The electric field gradient (EFG) q is calculated from a point-charge model of the distorted lattice. They found surprisingly good agreement for such a simple model. On the other hand, Bhide and Multani[29] used a point-charge and point-dipole model and also assumed 60% ionicity to get agreement between measurement and calculation for Fe^{3+} in $BaTiO_3$. Bhide and Multani[30] also studied the EFG for Fe^{3+}-O vacancy in $BaTiO_3$, but did not get agreement between the experimental and computed values. In general, the calculation of quadrupole splittings in systems where ionic positions are well known has not been successful[31] and we feel that such calculations for strongly distorted systems such as Mn-O vacancy in $KTaO_3$ are quixotic.

To complete the remarks on hyperfine structure, we note that the forbidden lines of the $(-\frac{1}{2}\rightarrow\frac{1}{2})_{\perp}$ sextet of Fig. 3 are in agreement with theory. These doublet splittings range from about 18 to 22 G and *increase* as the magnetic field increases. The coefficient $(3\cos^2\theta-1)$ of the fourth term of Eq. (2) explains the range and direction of the doublet splittings, i.e., the range is about 8 G for $\theta=0°$ and decreases with increasing field and is 4 G for $\theta=90°$ and increases for increasing field. To explain the "center-of-gravity" shift from ~14 to ~20 G we must use the third-order terms of Lyons and Kedzie.[27] The last term of Eq. (A12) of Ref. 27, for $\theta=90°$, yields $-12AD^3/H^3\simeq 5$ G. Note that the product AD must be negative to get the correct sign of shift. Therefore, A is negative as expected.

III. CONCLUSION

Our main result is that the EPR of Mn in $KTaO_3$ arises from divalent manganese at a single site, almost certainly the Ta site with an adjacent oxygen vacancy. We have also shown that the temperature dependence of the axial constant D correlates with the host falling mode frequency and have measured the nuclear quadrupole splitting. However, at present the calculations of D and the EFG are not reliable so that these experimental results cannot be used to learn such important lattice parameters as ion position and induced polarization.

ACKNOWLEDGMENTS

The author wishes to thank K. A. Müller and R. M. Macfarlane for helpful discussions on this paper, and T. Kuga for technical assistance. The author is also grateful to G. Wessel who kindly recorded the EPR between 32 and 38 GHz.

[1]D. M. Hannon (unpublished).
[2]A. W. Horning, R. C. Remple, and H. E. Weaver, J. Phys. Chem. Solids 10, 1 (1959).
[3]K. A. Müller, Helv. Phys. Acta 31, 173 (1958).
[4]L. Rimai, T. Deutsch, and B. D. Silverman, Phys. Rev. 133, A1123 (1964).
[5]K. A. Müller, W. Berlinger, and F. Waldner, Phys. Rev. Letters 21, 814 (1968).
[6]H. Unoki and T. Sakudo, J. Phys. Soc. Japan 23, 546 (1967).
[7]H. Ikushima, J. Phys. Soc. Japan 23, 540 (1967).
[8]H. Ikushima and S. Kayakawa, J. Phys. Soc. Japan

27, 414 (1969).
[9]M. Odehnal, Czech. J. Phys. 13, 566 (1963).
[10]R. Baer, G. Wessel, and R. S. Rubins, J. Appl. Phys. 39, 23 (1968).
[11]G. Wessel and H. Goldick, J. Appl. Phys. 39, 4855 (1968).
[12]R. G. Pontin, E. F. Slade, and D. J. E. Ingram, J. Phys. C 2, 1146 (1969).
[13]D. M. Hannon, Phys. Rev. 164, 366 (1967).
[14]E. Feher, Phys. Rev. 136, A145 (1964).
[14a]R. R. Sharma, T. P. Das, and R. Orbach, Phys. Rev. 149, 257 (1966).
[15]W. H. From, P. B. Dorain, and C. Kikuchi, Phys. Rev. 135, A710 (1964).
[16]See, for example, W. Low, *Solid State Physics* (Academic, New York, 1960), Suppl. Vol. 2.
[17]W. Reese has measured the heat capacity of Mn-doped $KTaO_3$ and finds the tail of a Schottky anomaly at low temperature. This anomaly is probably caused by the ground-state splitting of the Mn^{2+}.
[18]S. H. Wemple, Ph. D. thesis, MIT, Cambridge, Mass., 1963 (unpublished); W. A. Bonner, E. F. Dearborn, and L. G. Van Uitert, Am. Ceram. Soc. Bull. 44, 9 (1965).
[19]E. Simanek and K. A. Müller, J. Chem. Phys. Solids 31, 1027 (1970).
[20]W. M. Walsh, Jr., J. Jeener, and N. Bloembergen, Phys. Rev. 139, A1338 (1965).
[21]G. S. Bogle and H. F. Symmons, Proc. Phys. Soc. (London) 73, 531 (1959).
[22]W. I. Dobrov, R. F. Vieth, and M. E. Browne, Phys. Rev. 115, 79 (1959).
[23]G. Wessel (private communication).
[24]P. A. Fleury and J. M. Worlock, Phys. Rev. 174, 613 (1968); G. Shirane, R. Nathans, and V. J. Minkiewicz, *ibid.* 157, 396 (1967).
[25]R. R. Sharma and T. P. Das, J. Chem. Phys. 41, 3581 (1964).
[26]B. Bleaney and R. S. Rubins, Proc. Phys. Soc. (London) 77, 103 (1961).
[27]D. H. Lyons and R. W. Kedzie, Phys. Rev. 145, 148 (1966).
[28]Z. Sroubek, E. Simanek, and R. Orbach, Phys. Rev. Letters 20, 391 (1968).
[29]V. G. Bhide and M. S. Multani, Phys. Rev. 139, A1983 (1965).
[30]V. G. Bhide and M. S. Multani, Phys. Rev. 149, 289 (1966).
[31]For review, see A. Weiss, in *Proceedings of the Fourteenth Colloque Ampère: Magnetic Resonance and Relaxation, Ljubljana*, 1966 (North-Holland, Amsterdam, 1967), p. 1076.

PHYSICAL REVIEW B VOLUME 3, NUMBER 7 1 APRIL 1971

Theory of Hyperfine Properties of Liquid Metals – Application to Cadmium†

P. Jena* and T. P. Das
Department of Physics, University of Utah, Salt Lake City, Utah 84112

and

G. D. Gaspari‡
Department of Physics, University of California, Santa Cruz, California 95060

and

N. C. Halder
Department of Physics, State University of New York, Albany, New York 12203
(Received 8 July 1970)

A perturbation formulation is developed for the calculation of spin densities in liquid metals using nonlocal pseudopotentials. Specific application is made to liquid cadmium using experimental interference function data. The results explain the observed temperature independence of the Knight shift and nuclear-spin lattice relaxation time and provide empirical exchange-enhancement factors for these properties. A comparison is made with prediction of current exchange-enhancement theories and suggestions are made for improvement of the agreement between theoretical and experimental Knight shifts and relaxation times.

I. INTRODUCTION

A variety of experimental resonance data such as Knight shift K_s and nuclear-spin lattice relaxation time T_1 are becoming increasingly available for a number of liquid metals.[1–3] There appear to be three specific hyperfine effects associated with the data. Two of these, related to each other, are K_s and the relaxation rate $1/T_1$ due to the Korringa type of process, which is the only important one for spin-$\frac{1}{2}$ nuclei. The third property, namely, the nuclear quadrupole contribution to the relaxation rate,[3,4] requires a knowledge of the dynamics of the ionic motion in addition to the average ionic